Bridges et al., http://www.jcb.org/cgi/content/full/jcb.201512029/DC1

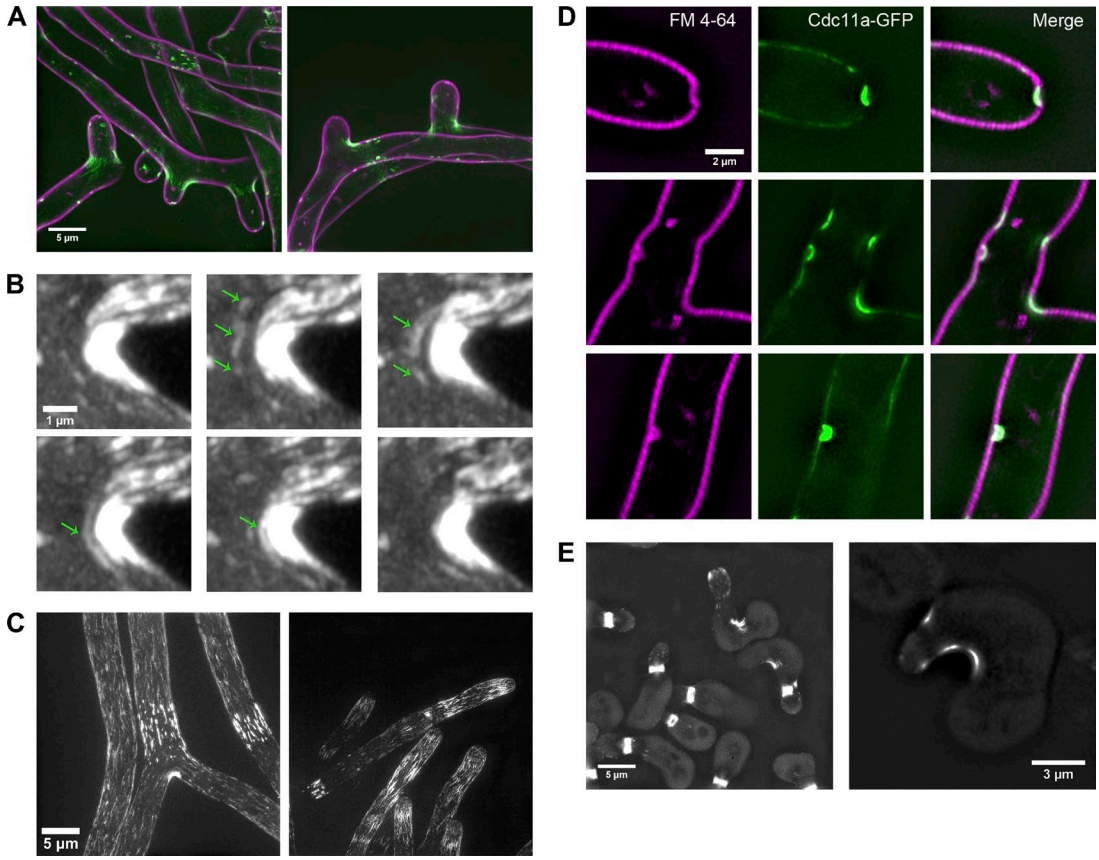

Figure S1. **Curvature-dependent septin localization in fungal cells.** (A) Colocalization of the *A. gossypii* plasma membrane (FM 4–64, magenta) and Cdc11a-GFP (green). (B) Septin filament annealing and addition to base of branch (arrows) visualized by Airyscan confocal microscopy. (C) Cdc11a-GFP visualization of septin filament orientation in areas that are devoid of positive curvature. (D) Addition of FM 4–64 (magenta), which alone stressed *A. gossypii*, resulted in tight membrane invaginations, to which Cdc11a-GFP (green) localized. (E) Localization of Cdc3-GFP in *S. cerevisiae* induced to shmoo by α factor addition.

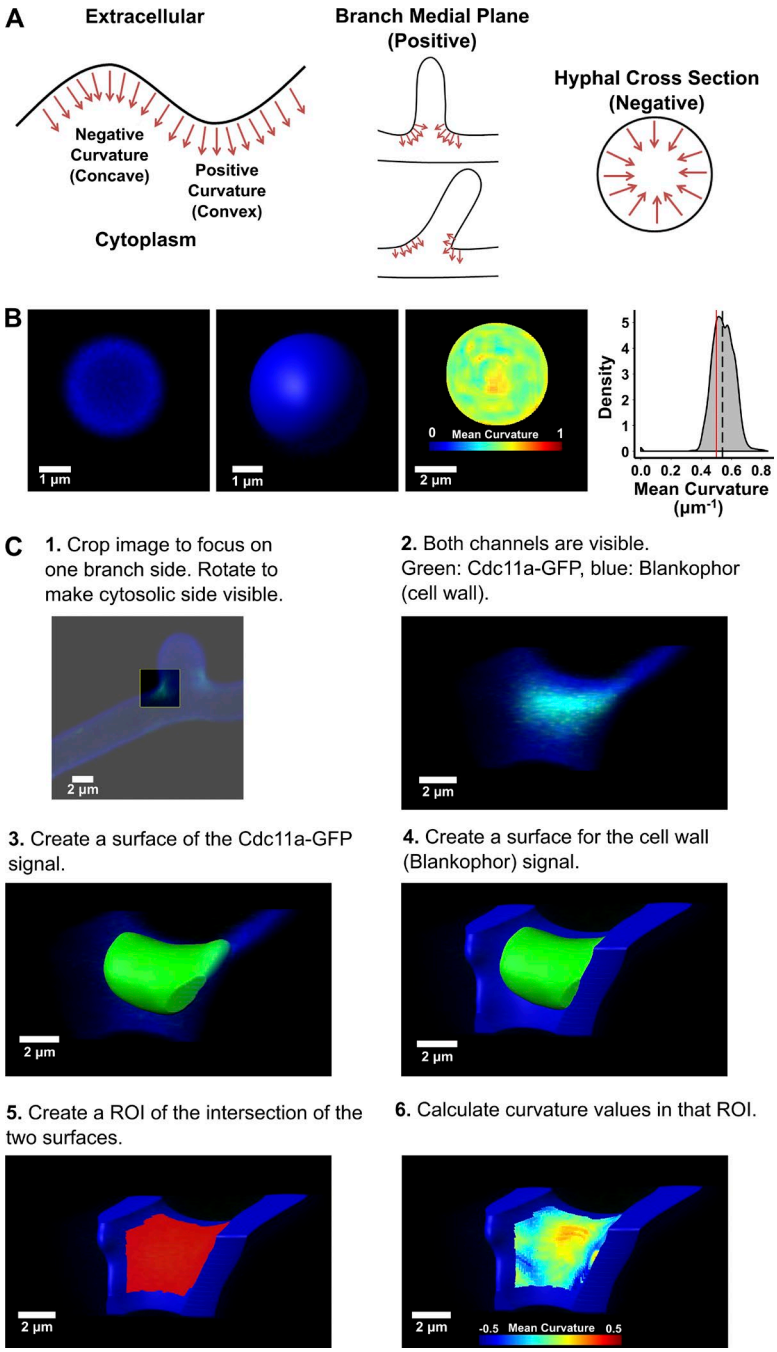

Figure S2. ***A. gossypii* curvature analysis.** (A) Graphical explanation of positive versus negative curvature as viewed from the cell interior. (B) To assess the accuracy of curvature measurements, curvature was measured of beads of known size. The red line denotes the expected curvature for a perfect 4-µm bead ($\kappa = 0.5\ \mu m^{-1}$); the dotted black line denotes the measured distribution mean ($\kappa = 0.54\ \mu m^{-1}$). (C) Workflow for analysis of curvature from the internal surface of *A. gossypii* cells.

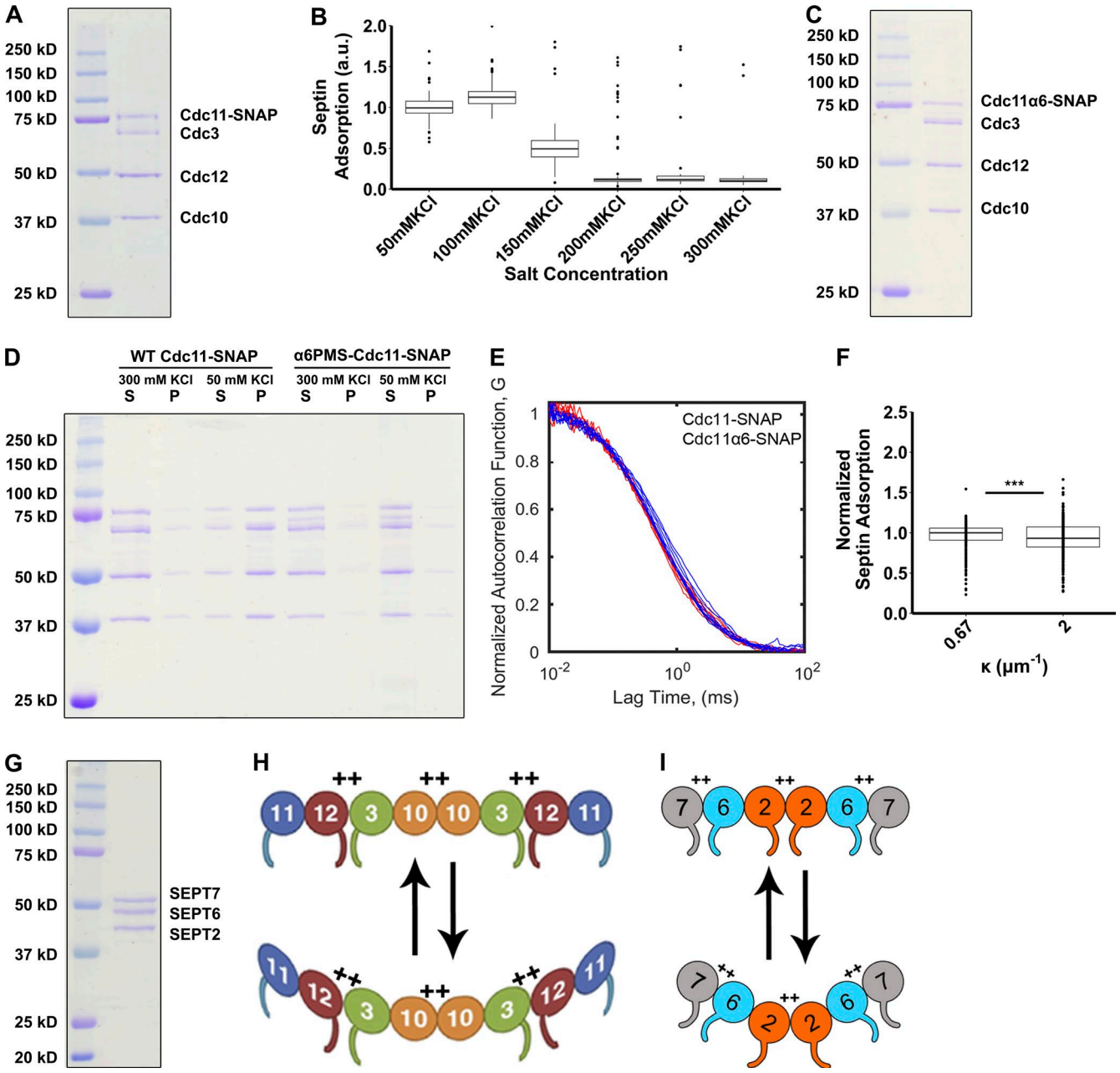

Figure S3. **Analysis of septin adsorption to bilayer-coated beads.** (A) Coomassie staining of recombinantly coexpressed and purified Cdc10, Cdc3, Cdc12-TEV-6HIS, and Cdc11-SNAP after removal of the 6xHIS tag by TEV protease. (B) Yeast septin adsorption to 1-μm bilayer-coated beads at 250-nM septin complex concentration at varying salt concentrations. $n \geq 39$ for each salt concentration. (C) Coomassie staining of recombinantly coexpressed and purified Cdc10, Cdc3, Cdc12-TEV-6xHIS, and Cdc11α6-SNAP after removal of the 6xHIS tag by TEV protease. (D) Pelleting assay of 500 nM WT–SNAP and Cdc11α6–SNAP complexes in high salt concentrations, which prevent polymerization, and low salt concentration, which promote polymerization of the WT complex. (E) Fluorescence correlation spectroscopy autocorrelation curves of WT–SNAP488 and Cdc11α6–SNAP488 complexes in 300 mM KCl. $n \geq 9$ measurements for each complex. (F) Normalized adsorption of 100 nM 6xHIS–GFP complexes to 1 μm ($\kappa = 2\ \mu m^{-1}$) and 3 μm ($\kappa = 0.67\ \mu m^{-1}$) beads containing 2% DGS-Ni^{2+} NTA lipids in 100 mM KCl. Although distributions were found to be different, 3 μm ($\kappa = 0.67\ \mu m^{-1}$) beads actually displayed a slightly higher mean septin adsorption. This trend was opposite to the trend observed with septins on the same bead sizes. We attribute the statistical difference to a large sample size (1-μm beads: 367 and 3-μm beads: 284), rather than a relevant experimental difference between the two bead sizes. For visualization of fold enrichment, data were normalized to 3-μm beads. (G) Coomassie staining of recombinantly coexpressed and purified SEPT2–6xHIS, SEPT6, and SEPT7–Strep complexes. (H) The yeast septin complex may arc, producing a complex that has a preferred geometric relationship with curved membranes. (I) Alternatively, the human septin complex has been shown to hinge in the middle, which could be the basis for curvature sensing. ***, $P < 0.005$.

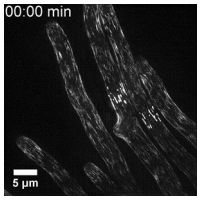

Video 1. **Cdc11a-GFP localization in *A. gossypii* during cell growth.** Entire z-series of endogenously tagged Cdc11a-GFP were acquired at 1-min intervals and are displayed as a maximum intensity projection. Images were acquired using structured illumination microscopy (DeltaVision OMX V4; GE Healthcare).

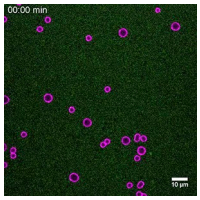

Video 2. **Septin dynamics in vitro on supported lipid bilayer–coated beads.** Septin adsorption (100 nM Cdc11–SNAP488 complexes, green) over time on a mixture of 3- and 5-µm beads coated in 75% PC, 25% PI, and trace Rh-PE (magenta) lipids. A single plane was acquired by simultaneous imaging of the two channels with 4-s intervals on a laser scanning confocal microscope (A1; Nikon).

Table S1. **Fungal strains used in this study**

Number	Description	Selectable marker	Source
AG384	ΔlΔt Ag*CDC11A*-GFP:GEN	GEN	Meseroll et al., 2013
AG376	ΔlΔt pAg*CDC11A*-GFP:GEN	GEN	This study
AG808	ΔlΔt pRS416-Ag*cdc11a*-α6-GFP:GEN	GEN	This study
AG809	ΔlΔt Ag*HSL7*-GFP-GEN:pRS416-Ag*CDC11*A-mCherry:Nat	GEN, NAT	This study
AGY036	GFP-Sc*CDC3*:Leu	LEU	E. Bi[a]

[a]University of Pennsylvania School of Medicine, Philadelphia, PA.

Table S2. **Plasmids used in this study**

Number	Description	Selectable marker	Source
AGB214	pAg*CDC11*A-GFP::GEN	amp	Meseroll et al., 2013
AGB849	pRS416-Ag*cdc11a*-α6-GFP::GEN	amp	This study
AGB141	pRS416-Ag*CDC11A*-mCherry:NAT	amp	DeMay et al., 2009
AGB710	pMVB128 6HIS-TEV-Sc*CDC12*/Sc*CDC10*	amp	This study
AGB501	pMVB133 pACYC-Duet Sc*CDC3*/Sc*CDC11*-SNAP	cam	This study
AGB744	pMVB133 pACYC-Duet Sc*CDC3*/Sc*cdc11*-α6PMs_E289R_Y291A_R292E-SNAP	cam	This study

Table S3. **Oligos used in this study**

Number	Sequence
AGO1557	5′-CATGGGCAGCAGCCATCACCATCATCACCACGAGAATTTGTATTTTCAGGGTAGCCAGGATCCGATGAGTGCTGCCACTG-3′
AGO1558	5′-CAGTGGCAGCACTCATCGGATCCTGGCTACCCTGAAAATACAAATTCTCGTGGTGATGATGGTGATGGCTGCTGCCCATG-3′
AGO172	5′-CCCGCGAAATTAATACGACTCAC-3′
AGO1192	5′-GCCTGATTCTGGACTTGAAC-3′
AGO1613	5′-CACACATGAGATATTATATCGAAGAGCTGAAACCGAGGCATTATC-3′
AGO1614	5′-GATAATGCCTCGGTTTCAGCTCTTCGATATAATATCTCATGTGTG-3′
AGO1609	5′-GGAACGAAGTCGTGTGAGAGAAAACCCAAGATTTAAAG-3′
AGO1251	5′-GAAATACTGGGTGGTGTAGG-3′
AGO1770	5′-GCTGTCTCTACCTCATCAATCC-3′
AGO1771	5′-TCCCGTGCCAAGTATGTATC-3′
AGO130	5′-GTACTTGCGCTCGCTACTTC-3′

The following scripts are provided online: filamentOrientation.m: Calculates filament angles with respect to branch angle; XT_MJG_MSJ_Curvature.m: Imaris XTension to calculate curvature values on an Imaris Surface and select curvature values within an ROI; and XT_ROI_part2_MSJ.m: Imaris XTension that complements XT_MJG_MSJ_Curvature.m by expediting the ROI selection process.

References

DeMay, B.S., R.A. Meseroll, P. Occhipinti, and A.S. Gladfelter. 2009. Regulation of distinct septin rings in a single cell by Elm1p and Gin4p kinases. *Mol. Biol. Cell.* 20:2311–2326. http://dx.doi.org/10.1091/mbc.E08-12-1169

Meseroll, R.A., P. Occhipinti, and A.S. Gladfelter. 2013. Septin phosphorylation and coiled-coil domains function in cell and septin ring morphology in the filamentous fungus Ashbya gossypii. *Eukaryot. Cell.* 12:182–193. http://dx.doi.org/10.1128/EC.00251-12